Chapter 2
Overview of Clinical Applications Using THz Pulse Imaging, MRI, OCT and Fundus Imaging

After establishing the technological aspects of the four different imaging modalities in the previous chapter, this chapter focuses on their biomedical applications. First, THz pulse imaging is discussed within the context of assessing tissue vascularization, tissue water content, and the possibility of developing molecular fingerprinting. A similar discussion of recent applications of MRI to bio-imaging is also provided. The complementarity of the two imaging methods is also highlighted. Finally, the use of fundus photography and OCT to perform disease diagnosis are also discussed.

2.1 Recent Advances in the Application of THz Pulse Spectroscopy to Biomedical Imaging

As discussed earlier, THz-TDS is a time-domain technique, where time gated reflections are analysed directly in the time domain by observing their attenuation, phase delay and temporal spread after interacting with matter. Their temporally good definition can provide localization of tissue interfaces on the basis of their different refractive index. Different tissues have a different frequency dependent refractive index. The real part of the refractive index is associated with the impedance mismatch of the excitation THz wave, whereas the complex part is associated with the absorbance. Studies in reflection geometry enable the indirect assessment of sample or layer thickness, and can be used to determine the position of embedded unknown objects, etc. [16, 24]. In addition to their relatively non-invasive interaction with biological tissue T-rays have significant potential in advancing both in vivo and in vitro biosensing applications [8, 16, 29]. Furthermore, a significant number of biomolecules have several characteristic 'fingerprint' resonances due to discrete molecular vibrational, torsional and librational modes, both in liquids and solids [4, 5, 30].

X. Yin et al., *Pattern Classification of Medical Images: Computer Aided Diagnosis*, Health Information Science, DOI 10.1007/978-3-319-57027-3_2

2.1.1 THz Radiation Absorption and Detection in Tissue

THz radiation interacts strongly with polar molecules, a prime example being water [2]. Polar water molecules are active in the infrared region and have various vibrational modes [3]. In the mid- to far-infrared, the vibrations involve combinations of the symmetric stretch ($\nu 1$), asymmetric stretch ($\nu 3$), and bending ($\nu 2$) of the covalent bonds. The vibrations of water molecules may be thought of as restricted rotations, resulting in a rocking motion, as shown in Fig. 2.1a. In liquid water, since hydrogen bonds are much weaker than the covalent bonds (intra-molecular), their bond lengths are much longer (1.97 Å versus 0.96 Å), as shown in Fig. 2.1b. Steric effects from dipole moments in water clusters vary according to hydrogen proximity and, as a consequence, shifts in ro-vibrational modes at THz frequencies are encountered. Furthermore, these shifts are expected to be loosely correlated with different water potential values, which indirectly affects molecule's ability to interact with its surrounding molecules. This has further important ramification on the way proteins influence the state of water. An analysis of steric forces can lead to further understanding of the function of hydration shells in proteins [17, 41, 42].

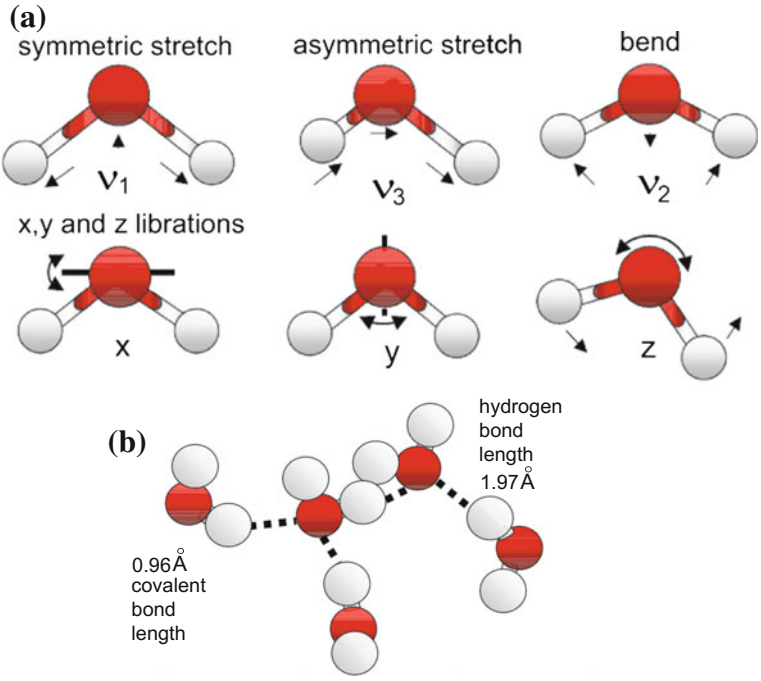

Fig. 2.1 **a** The main vibrational modes in water. **b** A schematic diagram illustrating the differences between intra- and inter-molecular bonding in water. After [3]

As discussed earlier, THz-TDS provides a direct measure of the real and imaginary components of tissue permittivity. A Debye relaxation model can be used to analyze the strong absorption of THz radiation in polar liquids at least up to 1 THz [5, 32]. This model can be directly related to the associated intermolecular dynamics.

Biological tissue is generally composed of polar liquids. Due to the exceptionally high absorption losses of polar liquids at THz frequencies and the low source power in TPI systems, it is difficult for the THz radiation to propagate through biological tissue along a substantial distance. However, the same high absorption coefficient that limits penetration in tissue also provides extreme contrast between samples at various degrees of water saturation [5]. This property has proven advantageous in the examination of the properties of water uptake and distribution in plants [6, 7], as well as in the evaluation of the severity of burns through the study of necrotic skin samples [8]. In addition, [9, 10] describe the application of TPI techniques for imaging of basal cell carcinomas (BCC) *ex vivo* and *in vivo*. Note that BCCs typically show an increase in absorption of THz radiation compared to normal tissue. This may be attributed to either an increase in interstitial water within the diseased tissue [13] or a change in the vibrational modes of water molecules through interactions with other functional groups. Systematic studies in tissue identification are reviewed in [5].

2.1.2 *Identification of Compounds with Complex Composition*

T-ray spectroscopic studies also provide complementary information on low-frequency bond vibrations, hydrogen bond stretching and torsions in liquids and gases with the lowest frequency modes associated with intermolecular motion [19, 22, 23], as illustrated in Fig. 1.1. The vibrational spectral characteristics of biomolecules, which lie in this range (wavenumbers between 3.3 and 333 cm^{-1}) make T-ray imaging systems a promising sensing modality for clinical diagnosis. Another advantage of performing spectroscopic investigations at this part of the spectrum is that many molecules have characteristic 'fingerprint' absorption spectra [16, 18], thus making T-ray imaging systems a promising sensing modality for clinical diagnosis. The identification of pure compounds using molecular signatures with THz-TDS systems, however, is still not straightforward because of the inherently broad spectral signatures in liquids and solids. Nevertheless, there is a growing number of multiple confirmed observations of particular resonant signatures that may be attributed to the presence of compounds in pure form [142]. Of particular relevance here is the growing interest in studying the conformational structure, binding states, and vibrational or torsional modes of proteins and oligonucleotides [131, 132] through the analysis of spectral features [133]. Different reflection or absorption signatures may also be attributed to a change of density or polarizability, and these can be further associated with a dehydration state, or a denaturing process which give rise to a new amorphous absorption band or a temperature related absorption band shift [24, 33].

Pulsed THz wave technology has been applied extensively in biosensing [4]. Many pioneering investigations in biomolecule characterization were performed by the Aachen group [136] and Jepsen's group [134]. These were followed by a rapid growth of investigations by other researchers worldwide [135, 137, 138]. An interesting example is that of an affinity biosensor monitoring of the binding between biotin and avidin molecules on supported membranes composed of biotin layers on a quartz surfaces treated with octadecanol, as proposed by Menikh et al. [139]. In that work, an amplified detection of biotin-avidin binding was very clearly observed through the dithering of the samples in a THz beam. This was attributed to the conjugation of agarose particles and avidin molecules and a change in contrast due to a change of the refractive index resulting from the chemical binding process [30, 140]. Avidin has a very strong affinity for biotin and is capable of being bound to any biotin-containing molecules. The importance of the work is that it showcases THz pulse sensing as a generic detection technique that can potentially be used to detect DNA hybridization and antigen-antibody interactions [30]. THz transient spectrometry has also been used to successfully distinguish between two artificial RNA single strands, composed of polyadenylic acid (poly-A) and polycytidylic acid (poly-C), from their different THz spectral transmission responses [17, 141].

The identification of pure compounds using molecular signatures with THz-TDS systems is still not straightforward because of the inherently broad spectral signatures in liquids and solids. Nevertheless, there is a growing number of multiple confirmed observations of particular resonant signatures that may be attributed to the presence of many compounds in pure form [142]. Of particular relevance here is the growing interest in studying the conformational structure, binding states, and vibrational or torsional modes of proteins and oligonucleotides [131, 132] through the analysis of spectral features [133]. Different reflection or absorption signatures may also be attributed to a change in density or polarizability, or may indicate a dehydration state, or a denaturing process leading to a new amorphous absorption band or a temperature related absorption band shift. A compilation of readily identifiable spectral signatures of complex biomolecules in an atlas has already been considered at Durham University, and significant progress has been made to include a significant variety of different tissue types. Yet there is a wider recognition by the THz community that this approach although very useful it is unlikely to have the universal applicability that can be found in other databases such as HITRAN, because of the variability in the location of the spectral bands observed. Such problems are further compounded by noting the variation in spectra of similar substances when these are recorded at different labs. Different sample preparation techniques and a lack of protocol standardization have been a problem within the THz community. Sample standardization which is normally found in the crystallographic community could be significantly beneficial in that respect.

In addition to the above, there are also other relevant studies based on frequency specific fingerprinting of biomolecules that have been discussed in the literature. Nishizawa et al. [144] illustrated the use of a widely tunable coherent THz scanning system for THz transmission spectroscopy to study samples consisting of nucleobases and nucleotides in crystalline form to further gain an insight of the composition of

RNA and DNA molecules. The THz spectra of those samples were measured in the 0.4–5.8 THz range. These studies showed that the molecules have quite different characteristic spectral patterns in this frequency region, furthermore, the absorption signature patterns observed were sufficiently clear and reproducible for identifying and discriminating between these molecules.

Using pulsed THz spectroscopy [31, 131], it has also been possible to study the low frequency collective vibrational modes of bio-molecules, i.e. DNA, Bovine Serum Albumin and Collagen in the range 0.1–2.0 THz. It is generally accepted that for most samples, broadband absorption increases with frequency and a large number of the low frequency collective modes for these systems is also deemed as IR active. Herrmann et al. [143] also carried out measurements of THz spectra of Poly(dA-dT)-Poly(dT-dA) DNA and Poly(dG)-Poly(dC) DNA and used new signal processing routines to infer the THz complex refractive index. The resultant spectral features showed that those samples were indeed distinguishable in the range 0.1–2.4 THz. Several research groups in Germany and Australia, have also studied the photo-isomerization of retinal chromophores [145, 146] focusing on the conjugated polyene chain of the biologically important chromophore retinal and its low-frequency torsional vibration modes. In that work, the absorption and dispersion spectra of different retinal isomers (all-trans; 13-cis; and 9-cis retinal) in the far-infrared region between 10 and 100 cm^{-1} were measured by THz-TDS at 298 and 10 K. At low temperatures, it was observed that the broad absorption bands resolve into narrow peaks that directly correlated to torsional modes of the molecule. The study also confirmed that vibrational modes within the molecule can be approximately localized through a comparison of the absorption spectra of different retinal isomers.

An alternative important research direction vigorously pursued by Teraview Ltd., Cambridge, U.K., aims to put an end to patent infringements within the pharmaceutical industry by detecting the presence of drug polymorphs [23, 147, 148]. Such studies, for example, have successfully used TPI to examine the variation in the crystalline structure of Ranitidine Hydrochloride polymorphs. Significant differences in the spectra of two different polymorphs were clearly observed at around 1.10 THz enabling their correct identification. A recent account on advances in the identification of the crystalline structure of drugs using TPI is provided in [149]. Furthermore, the observation of the crystallization of compounds has also been possible [150].

2.1.3 Recent Advances in the Application of DCE-MRI Imaging Techniques to Biomedical Imaging

MRI has proven to be of clinical importance to the classification, grading, and diagnosis of tumours. Clinical management of many tumour types is now reliant on MRI. Clinical information for both surgical planning and clinical management is derived from tumour morphology and the relationship of lesions to neighbouring structures that are revealed using MRI. Magnetic resonance provides images for clear identifi-

cation of some cases of pathological change, as well as delineation of organ location and the identification of anatomical features.

An evolution of this imaging modality since the 1980s has been an alternative high-performance imaging modality which is called dynamic contrast enhanced DCE-MRI. This is now widely used in the diagnosis of cancer and is becoming a promising tool for monitoring tumour response to treatment [151]. DCE-MRI patterns can be affected by a wide range of physiological factors; these include vessel density, blood flow, endothelial permeability and the size of the extravascular extracellular space in which contrast is distributed [151, 152]. The crucial difference from traditional medical imaging (i.e. X-rays) is that the DCE-MRI modality provides 3D spatial information about lesions as well as temporal information about lesion physiology (showing variations in contrast agent uptake rates), allowing for more accurate assessment of lesion extent and improved lesion characterisation [68, 89].

Typically, DCE-MRI images are acquired with the use of a conventional gradient echo (GRE) pulse sequences that repeatedly image a volume of interest after injecting a contrast agent, such as gadolinium diethylenetriamine pentaacetic acid (Gd-DTPA) into the patient's blood stream. The DCE imaging employs a full k-space sampling strategy, (where the k-space relates to the associated wavenumber, a terminology originally introduced by the semiconductor industry to denote momentum space but in MRI is associated with spatial frequency). Three dimensional (3D) volume acquisition of slice profiles is normally performed. These are generally rectangular and always contiguous slices. By registering slices in a contiguous manner, the signal is recorded and integrated uniformly from all tissue coordinates in each slice, thus avoiding cross-talk.

One of the biggest advantages of the gradient-echo pulse sequence is that it can be performed quickly enough to enable 3D FT (3DFT) data acquisitions. In 3DFT imaging, a volume or slab of tissue is excited, rather than merely a thin slice of tissue. This means the 3D MRI data acquisition consists of three different phase encoding directions: the transaxial plane, the sagittal plane, and the coronal plane. Images are obtained sequentially every few seconds over a period of up to 5 to 10 min. There is always a trade-off between spatial (sRes) and temporal (tRes) resolution. Usually, most radiologists clinical protocols show a preference for scans at high sRes allocating only 1–2 min for tRes data acquisition [153].

A typical DCE-MRI dataset consists of one baseline 3D MR image which is used as a reference before contrast agent injection [31, 62]. Additional scans are performed to acquire post-contrast images at the second, third, and subsequent slices (usually 6 or 7). Each time slice has a typical time interval of 60 s.

Following the terminology introduced independently by Ljunggren [154] and Twieg [155] we shall refer to the, k-space to denote the spatial (either 2-D or 3-D) frequency domain of the imaging system. Within the context of temporal image processing the k-matrix, is composed of digitized MR signals stored during the data acquisition process before any reconstruction computations. The complex data entries are associated with the pulse sequence of the accurately timed radio frequency and gradient pulses.

In clinical practice e.g. during a DCE-MRI mammogram, reducing the signal acquisition time is desirable, and this is normally achieved by undersampling the *k*-space. Undersampling may be achieved by adopting a random partial *k*-space updating [156] protocol. The HASTE sequence, which samples half the *k*-space [157], is now routinely used in clinical MRI.

Aliasing from sampling the k-space below the Nyquist rate, however, introduces imaging artifacts [385]. Since there is always a need for better tRes while preserving adequate SNR and sRes, several groups [158–160] have shown that it is possible to accelerate DCE-MRI (without employing parallel imaging) by a factor of ten using compressed sensing (CS) based for image reconstruction as proposed in [108]. The approach allows the filling of missing *k*-space data using a constrained optimization technique to interpolate the values between under-sampled adjacent data points in the spatial domain.

Recent work by Yin et al. [65] based on the broad principles of compressed sensing represents an important advancement in the above mentioned CS modality. The technique makes use of the fact that, when under-sampling the *k*-space, it is possible to use variable density sampling schemes in a Cartesian coordinate system to widely distribute the resulting artifacts and reduce their visual impact. Such an approach was further explored using a model-based method for the restoration of MRIs with sparsity representation in a transformed domain, e.g. spatial finite-differences (FD), or after using the discrete cosine transform (DCT). The reduced-order model, in which a full-system-response is projected onto a subspace of lower dimensionality, has been used to accelerate image reconstruction by reducing the size of the linear system associated with the measurement space. The singular value threshold technique [161] (SVT) was used in the denoising scheme to reduce and select the model order of the inverse FT image, and to restore multi-slice breast MRIs that have been compressively sampled in *k*-space. Restored MRIs with SVT de-noising show reduced sampling errors compared to direct MRI restoration methods via spatial FD, or DCT. The difference image related to IT, shown in Fig. 2.2b, contains a relatively large number of noisy (error) pixels that are located around the boundary of the imaged section. Reconstruction with the identity transform (IT) also shows some blurring at the image edges. In contrast, the reconstructed image using SVT denoising illustrated in Fig. 2.2a, shows a reduced number of error pixels compared to the reconstructed image in Fig. 2.2b.

2.1.4 Recent Advances in the Application of fMRI Imaging to Biomedical Imaging

Functional Magnetic Resonance Imging (fMRI) is a non-invasive imaging technique that does not require the injection of contrast agent [59]. Functional MRI has relatively high spatial and reasonable temporal resolution, and can be acquired in the same session as structural MRI. It effectively captures the changes in the Blood Oxygenation Level Dependent (BOLD) contrast, allowing the evaluation of brain

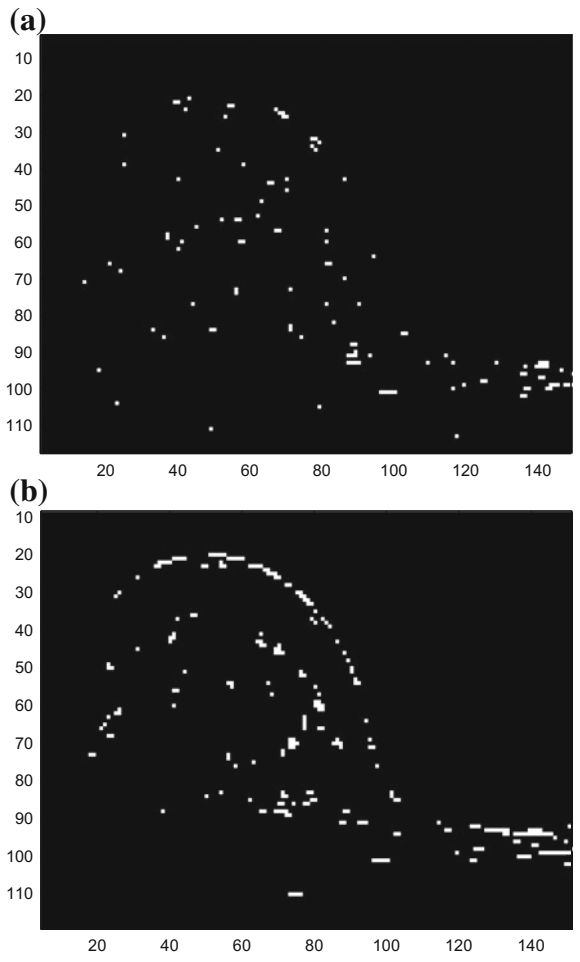

Fig. 2.2 **a** Illustration of the difference image segment between the measured MRI and reconstructed image using SVT for denoising. **b** The difference image segment between the measured MRI and transformed image from sampled k-space

activity due to external stimuli. The low signal-to noise ratio (SNR) of fMRI data makes detection of the activations-related signal changes difficult; hence most of the data is collected from periodic stimulation after alternating with the rest condition. The temporal dynamics of the activation response, which is delayed and is relatively slow compared to actual brain activity, is another problem that must be dealt with during analysis. Most of the present methods rely on exclusive modelling of the hemodynamic response function to detect this delayed activation. The most extensively used fMIR data analysis techniques are variants of the general linear models based on the t-test, the F-test, on correlation coefficients (between observed responses and stimulus function) or multiple linear regression. A general drawback in all these techniques is that they require accurate knowledge of the actual stimulus function.

At this point it is also worth noting that, in experimental NMR studies, the transverse magnetization decays at rates much faster than what would be theoretically predicted by natural atomic or molecular mechanisms; this accelerated rate is commonly denoted as T2* ('T2-star'). These T2* relaxations relate to the decay of transverse magnetization caused by a combination of spin-spin relaxation and magnetic field inhomogeneity. For this reason, the MR sequences obtained using gradient echoes and relatively long TE values are also called T2*-weighted. They are often used to accentuate local magnetic homogeneity effects to aid in the detection of hemorrhages or calcification. T2*-sensitive sequences also form the basis for functional MRI (fMRI) using the BOLD technique. From the above description it may be concluded that T2* is always less than or equal to T2.

Figure 2.3 illustrates the general principle of fMRI. Oxygen is delivered to neurons by haemoglobin in capillary red blood cells. When neuronal activity increases there is an increased demand for oxygen and the local response is an increase in blood flow to those regions of increased neural activity. Haemoglobin is diamagnetic when oxygenated but paramagnetic when deoxygenated. This difference in magnetic properties leads to small differences in the MR lifetime signal in the blood in that region according to its level of oxygenation. Since blood oxygenation varies according to the levels of neural activity, these differences can be used to spatially localise and temporally resolve brain activity. Brain fMRI BOLD imaging is one of the most promising emergent measurement modalities with several applications in neuroscience, neurosurgery, rehabilitation and psychology. An overview of recent advances of functional imaging in oncology can be found in the comprehensive book edited by Luna et al., (2014) [163]

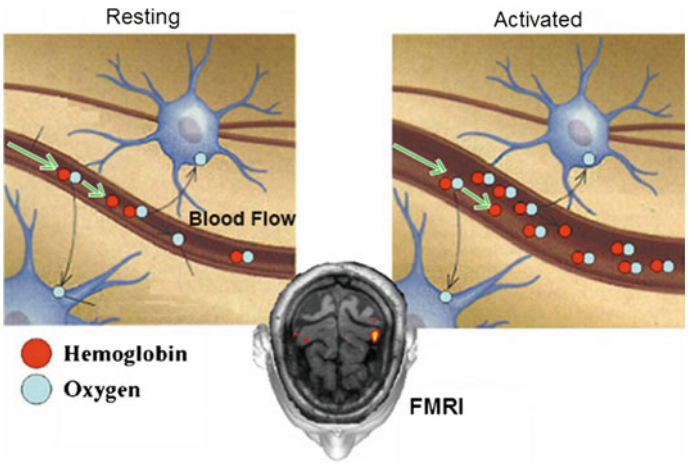

Fig. 2.3 Simplified illustration of different levels of oxygenation in blood on the basis of a resting or activation state of a nearby neuron as observed through fMRI. After [162]

2.1.5 *Advantages and Shortfalls of T-Rays and DCE-MRI & FMRI*

As TPI and MRI time series are becoming more widely available in conventional clinical practice, it is envisaged that data acquisition and analysis will be performed in tandem to benefit from the complementarity of each signal, thus capitalizing on the inherent differences in signal generation and tissue contrast mechanism. One of the primary advantages of THz imaging over MRI, is the availability of various spectroscopic signatures within a frequency band which may be attributed to changes of THz biomarker concentration.

Although, a number of papers discuss spectroscopic investigations of biomolecules such as DNA [4, 17, 131, 143, 144], unfortunately the responses of many biological tissues are unknown in this band. A further related problem is the current lack of development of reliable computer aided diagnostic algorithms for interpreting the multispectral images obtained by T-ray imaging [164]. A number of authors have partly addressed this question by fitting the measured data to linear models and using the filter coefficients as a means of classifying different tissue types [11]. One of the most important potential applications for THz technology along this line of research is the detection and identification of specific biological and chemical agents [165]. Although it is widely recognized that T-rays can be used to image tumour microvasculature, most reports focus on the feasibility of using TPI to image breast tumours [166, 167] and skin cancer [168]. In both these cases, the contrast observed is mainly due to the absorption of THz waves by the water that is present in biological tissue and the actual state of hydration of the tissue under study. A recent review carried out by Yu et al. [169], extensively discusses such investigations and relates them to the future potential of THz imaging and spectroscopy for performing cancer diagnosis. A further important development in THz tumour image analysis has been reported by Huang et al. [170], where gold nanorods were used in vitro as novel contrast agents for both molecular imaging and photothermal cancer therapy. With the aid of a laboratory microscope, those investigations showed that, as a result of the strongly scattered red light from gold nanorods in the dark field, malignant cells can be clearly visualized and identified from non-malignant cells.

As THz time domain spectroscopy (THz-TDS) and imaging are being extended to address new biomedical problems, the identification of specific proteins is likely to be the focal point in those investigations. Such research direction can draw upon previous investigations on histo-morphology studies of healthy and diseased excised tissue [171, 172]. Lyophilized tissue samples from various organs have also been imaged [173] and this approach has the advantage of eliminating the effects of water absorption thus providing a more reproducible THz signature by eliminating the variability commonly present in various levels of hydration of the sample. A good application example for such investigations would be the study of the collective vibrational modes of protein deposits found in amyloidosis. In humans, the accumulation of protein deposits in tissue occurs as part of the natural ageing process. An unnaturally rapid accumulation of deposits, however, can occur in diseases such as

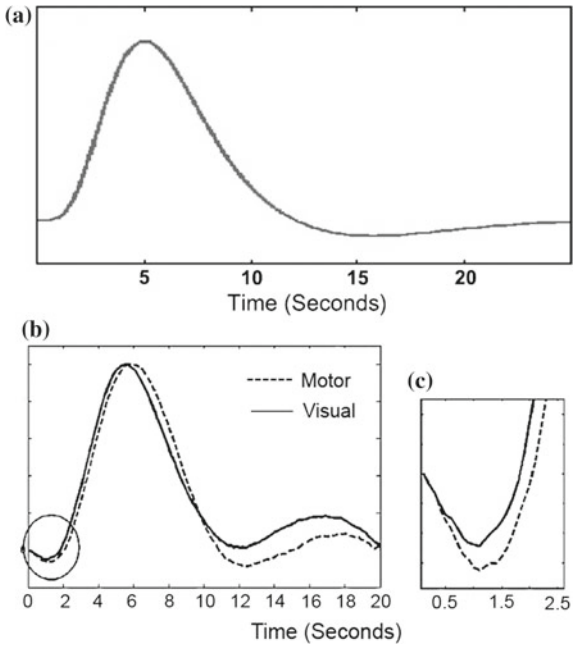

Fig. 2.4 **a** The standard canonical model for the HRF used in fMRI data analysis illustrates the main features of the response. **b** Examples of empirical HRFs measured over the visual and motor cortices in response to a visual-motor task. **c** The initial 2 s of the empirical HRFs give strong indication of an initial decrease in signal immediately following activation. After [175]

Alzheimer's Disease (AD), resulting in the functional decline of the tissue, leading to dementia. This is a particularly promising research direction for THz spectroscopy investigations as the early detection of AD can lead to a much better management of the disease.

Furthermore, as mentioned earlier, fMRI is often used to identify brain areas activated by a stimulus. The observed change in the fMR signal, however, is the result of an indirect effect related to the changes in both blood flow rates as well as level of oxygenation following changes in neural activity. The underlying evoked hemodynamic response to a neural event is typically referred to as the hemodynamic response function (HRF). Figure 2.4 shows the typical shape of such a curve after modelling the HRF; this is sometimes also called the canonical HRF. The increased metabolic demands due to neuronal activity lead to an increase in the inflow of oxygenated blood to active regions of the brain. Since more oxygen is supplied than actually consumed, this leads to a decrease in the concentration of deoxyhemoglobin which, in turn, leads to a small, but measurable, signal increase because deoxyhemoglobin is paramagnetic.

When considering the complementarity between BOLD-fMRI and THz-TDI in the above example, it is worth noting that the BOLD-fMRI modality is correlated to both levels of hemoglobin oxygenation as well as flow rate, and an independent measurement of water content spatially resolved using THz-TDI can enable a better differentiation between the two signals. This becomes particularly useful, for example, when standard diffusion tensor models are deemed inaccurate.

From the perspective of both spatial and temporal resolution, the two techniques are complementary to each other [175]. In fMRI, it is impossible to simultaneously increase both, as increases in temporal resolution limit the number of k-space measurements that can be made in the allocated sampling window and thereby directly influence the spatial resolution of the image. Unlike conventional enhanced MRI, which simply provides a snapshot of enhancement at one point in time, DCE-MRI permits a more complete depiction of the wash-in and wash-out contrast kinetics within tumors. Signal intensity data are often normalized to concentration prior to analysis [174].

THz measurements with femtosecond transients of tumours produces significantly different signatures to those produced when imaging normal adipose (fatty) tissue [11, 12]. Such differences may be attributed to the absorption coefficient and refractive index of each tissue. Similarly, changes in signal intensity taken from DCE-MR images are different for healthy and tumour tissues according to the different degree of absorption of the contrast agent. A further difference between the two datasets stems from the fact that DCE-MRIs are typically acquired at several time frames. This process is associated with a restricted temporal resolution.

2.1.6 Combining MRI with Alternative THz Spectrometric Systems and Other Imaging Modalities

2.1.6.1 Alternative THz Spectrometric Imaging Modalities for Biomedical Applications

Over the years, several alternative THz systems to the ones described in Sect. 1.1 have also been proposed [176–181], and these may also form the basis of THz spectrometric systems which can eventually be combined with MRI or fluorescence imaging modalities. Of particular note in such systems are the spectrometers based on the asynchronous optical sampling (ASOPS) scheme [182–185]. The technique uses two pumped femtosecond Ti:sapphire ring oscillators which produce femtosecond pulses with a repetition rate f and $f + \Delta f$ as set by the optical path length of each resonator (around 1 GHz when free running). Using beam splitters, a small portion of the signal (ratio 90:10) is directed to fast photodiodes which produce electrical trigger signals which are further amplified by low-noise high bandwidth microwave amplifiers (e.g. model ZFL 1000LN from Mini-circuits) operated in a trans-impedance configuration (converting a photo-current into a voltage). Although the photodetectors are not preserving the shape of the pulse, this is of no consequence to the stabilization scheme as the goal is to just generate a triggering event for the synchronization process. The difference in repetition rate ($\Delta f \approx 10$ kHz) is obtained using a microwave mixer and the signal is subsequently sent to a frequency-to voltage converter which serves as an input to a proportional integral derivative (PID) controller that drives the piezoelectric transducer that controls the path length in the slave resonator cavity. Figure 2.5 illustrates the asynchronous optical sampling scheme.

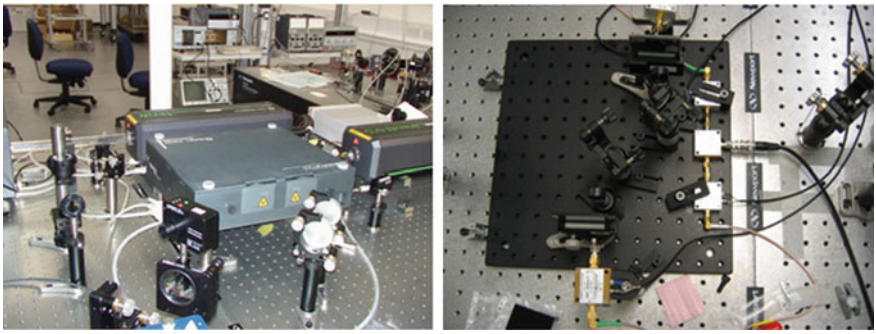

Fig. 2.5 ASOPS spectrometer and external frequency difference stabilization scheme that controls the repetition rate of the slave ring laser resonator to be always offset by a small amount e.g. 10 kHz to that of the master laser resonator

The close-loop system has a large linear gain in the forward path (composed of the cascaded PID signal, high voltage amplifier signal, the transducer voltage to displacement conversion, and the conversion of resonator path length to frequency comb repetition rate) and unity gain in the feedback path. With reference to Fig. 2.6, using transfer function notation and using $A \gg 1$:

$$V_{\text{out}} = \frac{A}{1 + AB} V_{\text{REF}} \approx \frac{A}{AB} V_{\text{REF}} = \frac{V_{\text{REF}}}{B} \tag{2.1}$$

so that the characteristics of the system are governed by the stable characteristics of the feedback path B. The difference in the repetition rate between the two resonators is set by V_{REF}. More recently, an alternative version of that system (TL-1000-ASOPS) incorporating substantially improved locking between the two femtosecond resonator lasers as well as carrier envelope phase stabilization options, have been made available by Laser Quantum Ltd to complement their HASSP-THz system. The bandwidth of this spectrometer is up to 6 THz when operated with their proprietary Tera-SED planar large-area GaAs based photo-conductive emitters.

An important advantage of eliminating the translation stage from the spectrometer is that the spot size of the optical beam propagating through the reference path of the interferometer is no longer of variable size (due to diffractive spreading of the infrared beam) for different path lengths imposed by the translation stage, as is in the case for a conventional THz transient spectrometer. This is a very important advantage in ASOPS as a dilution of the gate pulse in an Auston receiver changes its multimoded antenna pattern in both amplitude and phase delay. This type of error has not been systematically addressed by the THz community although careful work [186] has shown that changing the spot size dramatically alters the recorded time-domain signature and hence the corresponding Fourier transformed spectrum. Such errors are endemic to most THz transient spectrometers and can be exacerbated

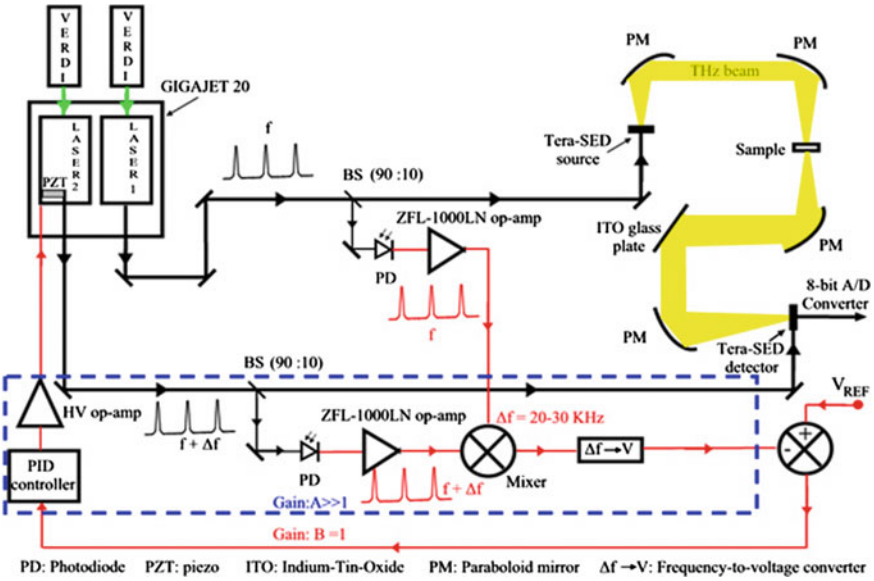

Fig. 2.6 Explanation of the feedback locking scheme found in ASOPS THz transient spectrometers currently marketed by Laser Quantum Ltd. Adopted from [185]

when ratioing the background and sample spectra. This is particularly important when interpreting spectra from imaged biological tissue.

An interesting alternative to the above scheme for the 9–12 μm part of the spectrum that may also be combined with other imaging modalities is that proposed by Keilmann's group (2004) [201, 202]. In this technique, the mid-infrared radiation from two electromagnetic waves (femtosecond duration pulses) is focused onto 0.5 and 1 mm GaSe crystals respectively, and through second order non-linearity 2 pulses whose overlapping bandwidth is centered at different frequencies is obtained. The two outputs of slightly different frequency are then superimposed to interfere on a power detector as shown in the figure below. A ZnSe combiner is used to direct the two beams to the detector and the down-converted signal is captured by a fast HgCdTe detector. The detector output signal contains a modulation ("beat") at the difference frequency Δ, which is conveniently selected to lie at the RF part of the spectrum (the technique is also known as multi-heterodyne spectroscopy), i.e. $f_r' = f_r - \Delta$. Interference modulation is produced by each heterodyne element. All modulations together may be viewed as a time-domain interferogram, that when Fourier transformed in the frequency domain, results in a harmonic radio frequency comb spectrum that is an exact replica of the dual beam's spectrum. A particularly attractive feature of the technique is that it can provide video-rate chemical imaging. Figure 2.7 illustrates the general principles of frequency comb spectrometry.

Such systems may also be further modified to perform imaging at subwavelength scale using near-field microscopy by observing the elastic light scattering from a tip

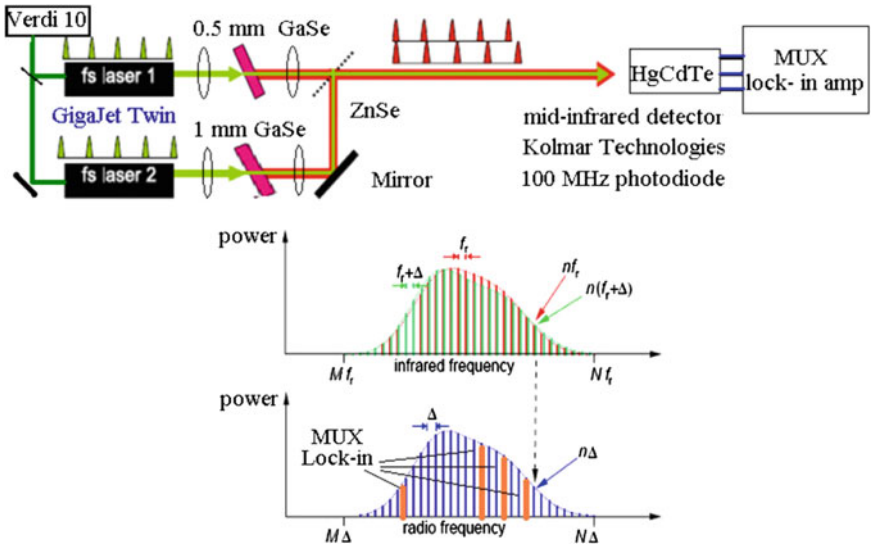

Fig. 2.7 Frequency comb spectrometry where a beat frequency signal at the RF part of the spectrum is generated after heterodyning the femtosecond pulses of two lasers (these are offset by a few Hertz). Multiplexed (MUX) lock-in amplifiers are subsequently used to select specific signatures for further chemometric analysis. After [202]

[188–191, 201]. The s-SNOM technique which provides vibrational contrast especially in the mid-infrared fingerprint spectral region, uses a light focused beam to illuminate the tip region of an atomic force microscope (AFM). By recording the scattered light in the backward direction, an optical image is simultaneously generated. The tip oscillates at the cantillever's mechanical resonance frequency (trapping mode) with the important consequence that the near-field optical image becomes modulated at the cantillever's resonance harmonics allowing electronic filtering against otherwise overwhelming scattering coming from the shaft and cantilever.

2.1.6.2 Combining MRI with THz and Other Imaging Modalities

The case for adopting a dual MRI-THz modality has been made clear in the seminal works by Oh et al. [192] as well as Park et al. [57], where the authors applied the technique to detect the onset of ovarian cancer. The diagnostic performance of such imaging has been significantly enhanced by the use of nanoparticle probes (NPPs). Multimodal probes enable the combination of various imaging techniques. THz waves for example, can efficiently interact with surface plasmons (SPs) associated with the injected nanoparticles. Such interactions are of a polaritonic nature. Polaritons are the product of combining an exciton (a bound state of an electron and an electron-hole which are attracted to each other by the electrostatic Coulomb

force) with Planck's energy-frequency relation. A surface plasmon polariton (SPP), therefore, is an electromagnetic wave that propagates along the interface between a metal and a dielectric; it is thus coupled to a charge density oscillation in the metal. The imaginary part of the wave's transverse wave vector attenuates the wave amplitude perpendicular to the interface, so that the wave is confined near the interface. The wave also extends a finite distance into the metal so that it propagates with both loss (ohmic losses in the metal) and dispersion. Thus, the most strongly bound SPPs are also the most lossy ones.

In the visible and near-infrared regions, where many common metals have relatively large resistivities, the interaction between the wave and the electron plasma is very strong, and hence the propagation distance is relatively short. At the microwave and radio-frequency regions, however, where metallic resistivity is typically extremely low, this interaction is very weak. Such plane waves propagating parallel to the interface are often referred to as surface waves, and do not have a plasmonic character. In the case of THz frequencies, which lie between the microwave and infrared parts of the spectrum, the interaction between the electromagnetic mode and the electrons in the metal are stronger than in the microwave range, but weaker than in the infrared region. This gives rise to several unique possibilities for medical imaging. For example, if a metal surface of an injected nanoparticle is curved, a significant fraction of the propagating THz wave will follow the curving metal. This is in contrast to the case in the microwave region, where almost none of the electromagnetic energy of a surface wave follows the curved surface. Furthermore, THz SPPs can have propagation distances of hundreds or thousands of wavelengths, whereas SPPs at higher frequencies typically have propagation lengths of only a few tens of wavelengths. If near-infrared (NIR) excitation of NPPs targeted to cancer cells is used, SPs around the nanoparticles will be generated, increasing the temperature of the water inside the cells, inducing a change in the THz signal. The combination of THz waves and NPPs, and the use of differential detection techniques, can thus result in more accurate imaging of cancerous tumours with high sensitivity. The excitation of localized nanoparticles with waves of different electromagnetic frequencies, can, therefore, provide complementary information which can assist clinicians in more accurately establishing the boundaries of different type of tissue. Furthermore, they may provide an assessment of molecular and cellular activities.

A typical example of such a multifunction probe is that of $Feridex^{®}$ (Gurbet Group, Paris, France), superparamagnetic iron oxide nanoparticles (SPIOs). When these are used, they can enhance the magnetic resonance image contrast by reducing the RF relaxation time of the water protons. $Feridex^{®}$ SPIOs consist of a metallic nanoshell with a core size of 10–15 nm which is coated with dextran (to improve MRI by helping the nanoshell travel in the body). These particles, however, can also be utilized as a contrast agent for THz imaging, following induction of SPs by an NIR laser. Figure 2.8 illustrates the response of a SPIO to a THz pulse and an RF pulse.

This type of system follows other recent trends in combining multiple imaging modalities for the early detection of cancer; for example MRI with fluorescence imaging as discussed by Lee et al. [193] or positron emission tomography with near-

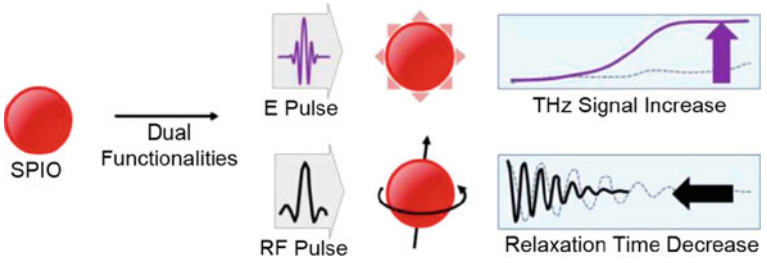

Fig. 2.8 Response of a SPIO to a THz pulse and an RF pulse. The SPIO has two functionalities, firstly it reduces the relaxation time of water protons in response to RF pulses in a strong magnetic field and raises the THz signal amplitude through SPs induced on the SPIO surface when exposed to an electric field. The magnetic feature is used for MRI and the electrical feature is used for THz imaging. After [57]

infrared fluorescence to characterize tumour vasculature as discussed in the work by Cai et al. [194], which combines positron emission tomography with fluorescent semiconductor nanocrystals (quantum dots) [195]. The use of quantum dots has significant advantages over their conventional organic fluorophore counterparts in that they have reduced photo-bleaching and a broad excitation spectrum with a narrow emission spectrum (with a sharp well-defined symmetric emission peak as opposed to a red tail) [196–199]. The resulting fluorescence is thus 10–20 times brighter so the associated images have better signal to noise ratio. A further advantage is that they have a large Stokes shift (difference between peak absorption and peak emission wavelengths) which reduces auto-fluorescence thus increasing sensitivity and clarity of the resulting images [200]. Because such nanocrystals can also be tailor-made to various sizes and shapes (which enables them to emit at different frequencies) their active uptake to different compartments in a cell can be identified and visualized simultaneously using wavelength multiplexing techniques [203–205]. Their inorganic composition also makes them more robust toward metabolic degradation which contributes to their longevity in vivo [206]. The multi-colour emission property of quantum dots allows the use of many probes to track several targets in vivo simultaneously [207, 208]. Furthermore, the yield obtained from quantum dots is almost 90% at room temperature [209]. Finally, they can also be easily functionalized [210]. An alternative is also to use lanthanide ion metal coordination complexes as luminescent molecular probes e.g. Yb(III), Er(III) and Nd(III) Eu(III) and Tb(III) complexes [211].

Following a critical review of MRI's ability to detect ovarian tumours [212], the need for imaging modalities with improved sensitivity has been established. The use of multifunction magnetic nanoparticles not only improves contrast in imaging [193], but also provides new opportunities for localized drug delivery [213, 214]. Furthermore, it opens-up the possibility of gaining further understanding of the biophysical environment and metabolic properties of the targeted cells [215]. The general idea of further combining multiple imaging modalities which can provide complementary information to existing imaging techniques is a rapidly evolving research topic that merits future exploration. For example, one could envisage that 2-photon microscopy

[217, 218, 222] could be combined with THz transient spectrometry since the femtosecond laser, used to create the seed pulses for the 2-photon system, can also be used at the same time to generate the pulses for the Auston switch or non-linear crystal for THz generation. Fluorescence lifetime imaging is a particularly useful experimental modality to the biomedical community as the de-excitation lifetime of the excited molecules is proportional to their concentration. Near-infrared radiation used in two-photon excitation suffers from significantly less absorption in biological specimens than UV or blue-green light, making the technique more appropriate for imaging thick specimens. The gradual loss in intensity (or 'attenuation') of excitation light from scattering is also reduced, as scattering decreases with decreasing excitation frequency. The technique can be label free and can rely on the natural fluorescence of compounds within the cell, so no additional dyes or quantum dots need to be added for the measurements. This can have important advantages since the physicochemical environment of the cells is not altered during the measurement process. Furthermore, because the technique relies on the use of short duration pulses for the excitation, there is less photo-bleaching of and photo-damage to the cells. The associated pulses may also be used for simultaneous chemical photoactivation or the activation of optogenetic switches. A further advantage of 2-photon microscopy over confocal microscopy is that it achieves confocality by using the emission pinhole aperture to reject out-of-focus light. However, inside thick specimens, scattering of the fluorescent photons is inevitable, resulting in significant loss of photons at the confocal pinhole. Two-photon microscopy limits the excitation volume, requiring no pinhole aperture, thus minimizing signal loss.

Alternative imaging modalities include variances of the well-known electron spin resonance (ESR) technique. The theoretical basis of ESR spectroscopy is similar to that of nuclear magnetic resonance (NMR), except that an electron spin, rather than a nuclear spin, is the focus [219]. Unpaired electrons in biological systems are in much lower abundance than nuclei, so ESR is a technique that focuses on local sites while NMR is more global. When biomolecules exhibit paramagnetism as a result of unpaired electron spins, transitions can be induced between spin states by applying a magnetic field and then supplying electromagnetic energy, usually in the microwave range of frequencies.

The interaction of an external magnetic field with an electron spin depends upon the magnetic moment associated with the spin, and the nature of an isolated electron spin is such that two and only two orientations are possible. The application of the magnetic field thus provides a magnetic potential energy which splits the spin states by an amount proportional to the magnetic field (Zeeman effect), and then radio frequency radiation of the appropriate frequency can cause a transition from one spin state to the other. The resulting ESR absorption spectra (also known as electron paramagnetic resonance (EPR) spectra) can be particularly useful to the study of radicals. This is because radicals typically produce an unpaired spin on the molecule from which an electron is removed. ESR is particularly suitable for studying basic molecular mechanisms in membranes and proteins by using nitroxide spin labels. In particular, nitroxide spin label studies with high-field/high-frequency ESR and two-dimensional Fourier transform ESR enable one to accurately determine distances in

biomolecules, unravel the details of the complex dynamics in proteins, characterize the dynamic structure of membrane domains, and discriminate between bulk lipids and boundary lipids that coat transmembrane peptides or proteins [220]. The semiconductor community has already combined an ASOPS THz transient spectrometer with a high magnetic field pulser for the characterization of materials [221]. It is therefore, appropriate to consider in the near future the adaptation of such a set-up to perform spectrometry of biomolecules.

Finally, it is worth mentioning the new opportunities to study biomolecules using dynamic nuclear polarization (DNP) techniques which increase the sensitivity of NMR spectroscopy by using high frequency microwaves to transfer the polarization of the electrons to the nuclear spins. The enhancement in NMR sensitivity can amount to a factor of well above 100, enabling faster data acquisition and greatly improved NMR measurements. With the increasing magnetic fields (up to 23 T) used in NMR research, the required frequency for DNP falls into the THz band (140–600 GHz) [223, 224].

2.1.7 Recent Advances in the Application of the Fundus Camera to Disease Diagnosis

As stated earlier, a fundus camera or retinal camera is a specialized low power microscope with an attached camera designed to photograph the interior surface of the eye, including the retina, retinal vasculature, optic disc, macula, and posterior pole (i.e. the fundus). The fundus enables direct observation of microcirculation non-invasively [225].

Many important eye as well as systemic diseases manifest themselves in the retina [119, 226, 227]. Changes in microcirculation can damage the retina. Assessment of vascular characteristics plays an important role in various medical diagnoses, such as diabetes [267, 268] hypertension [269] and arteriosclerosis [270]. Since the retina is normally not illuminated internally, external illumination projected into the eye, as well as the light reflected by the retina, must traverse the pupillary plane. Thus, the limited size of the pupil and the small opening in the iris (usually between 2 and 8 mm in diameter), has always been the primary technical challenge in fundus imaging [119]. Fundus imaging is further complicated by the fact that the illumination and imaging beams cannot overlap because this results in corneal and lenticular reflections, which tend to diminish image contrast. Consequently, separate paths are used in the pupillary plane resulting in optical apertures of the order of only a few millimeters. Because the resulting imaging setup is technically challenging, fundus imaging historically involved relatively expensive equipment and highly trained practitioners. Over the last ten years or so however, there has been a major effort to make fundus imaging more accessible, resulting in a reduced dependence on personnel expertise. This has also contributed to the wider proliferation of the technique.

One of the main applications for the fundus camera is in diagnosing microcirculation problems when the flow of blood in the smallest blood vessels in the network become blocked [225]. These changes in microcirculation can damage the retina. The

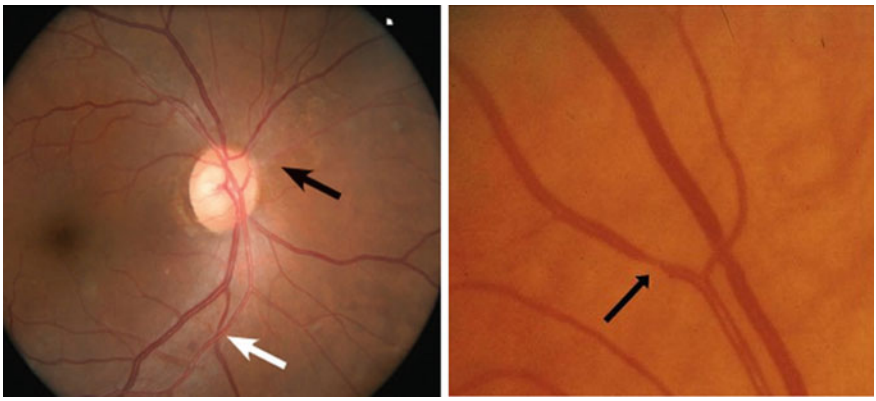

Fig. 2.9 (*Left panel*) Mild hypertensive retinopathy: generalized and focal arteriolar narrowing (*black arrow*) with arteriovenous nicking (*white arrow*). After [272]. (*Right panel*) An example of focal arteriolar narrowing. After [273]

abnormalities seen on a retinal image can be divided into two groups, those related to vascular changes and those related to extravascular changes. Both abnormalities can be used to predict the onset of hypertensive retinopathy, diabetic retinopathy, or a minute stroke. In addition there are features that are well correlated with anemia. Retinal arteries subjected to chronic hypertension show areas of focal or generalized narrowing. The light reflex is also narrowed. The arterial wall also thickens and becomes less transparent. As illustrated in the left panel of Fig. 2.9, mild hypertensive retinopathy shows generalized and focal arteriolar narrowing (black arrow) with arteriovenous nicking (white arrow). The right panel of Fig. 2.9 shows a retinal image with significant focal arteriolar narrowing.

A hallmark of diabetic retinopathy has been the identification of microaneurysms. Such a case is illustrated in the left panel of Fig. 2.10. The condition is characterized by tiny, round, red spots commonly seen in and around the macular area. These spots correspond to minute dilations of very small retinal vessels; the vascular connections are too small to be seen with an ophthalmoscope. In the right panel of Fig. 2.10, a case of non-proliferative diabetic retinopathy is illustrated. In the superior temporal quadrant, one can observe a large retinal hemorrhage between the two cotton-wool patches, this is accompanied by some beading of the retinal vein just above them, and by the presence of tiny tortuous retinal vessels above the superior temporal artery.

Stroke affects many elderly people, and sadly is a leading cause of death and disability. A simple and non-invasive method that predicts risk of stroke and stroke mortality which has been investigated developed by The Centre for Vision Research at Sydney University's Westmead Millennium Institute involves the use of fundus photography of the retina. An image that simultaneously shows the onset of a microaneurysm, the narrowing of retinal vesicles and athero-venous nicking which is typical of a patient who might have a stroke in the near future is illustrated in Fig. 2.11.

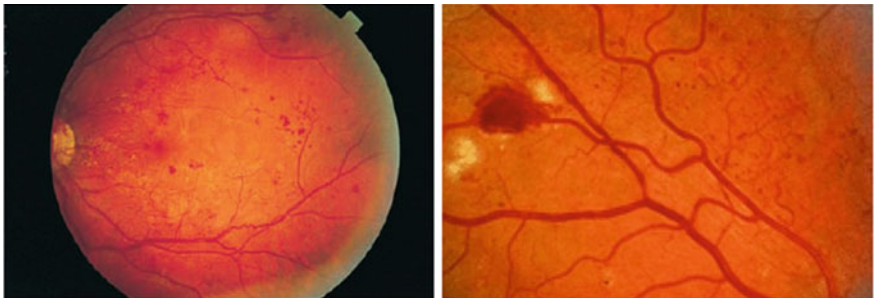

Fig. 2.10 The *left panel* shows tiny, round, *red* spots commonly seen in and around the macular area, which are the hallmark of diabetic retinopathy. The image on the *right panel* depicts nonproliferative retinopathy related to severe diabetic retinopathy. After [272]

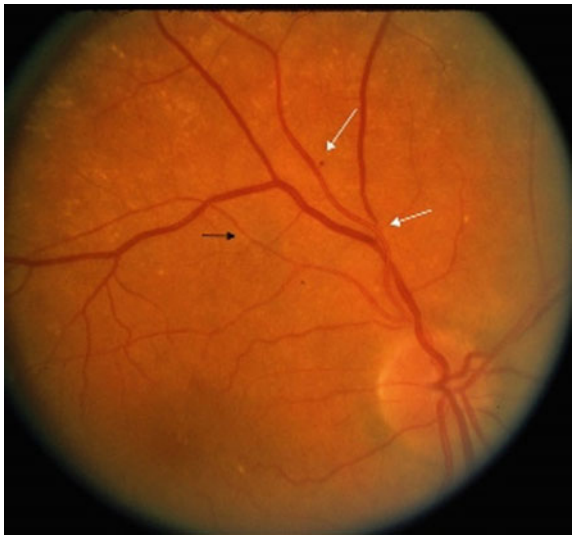

Fig. 2.11 A retina showing patient predisposition to stroke—The arrows indicate (clockwise from the *top arrow* in the picture). *White arrow* 1—A micro-aneurysm/haemorrhage; *Black arrow*—Narrowing of retinal vesicle; *White arrow* 2—Athero-venous nicking

2.1.8 Recent Advances in the Application of OCT Techniques to Disease Diagnosis

Optical coherence tomography (OCT) [232] has been used in a wide range of biomedical applications. [233, 234] OCT noninvasively acquires high-resolution, cross-sectional images of the retina [235]. A time-domain OCT system, such as the Stratus OCT device (Carl Zeiss Meditec, Dublin, CA), is capable of acquiring OCT reflectivity data at a rate of 400 axial scans per second. In addition, spectral-domain OCT (SD-OCT) systems, such as the Cirrus HD-OCT (Carl Zeiss Meditec) for example, have recently gained U.S. Food and Drug Administration approval. SD-OCT technology improves on time-domain systems, allowing performance of up to 27,000 axial

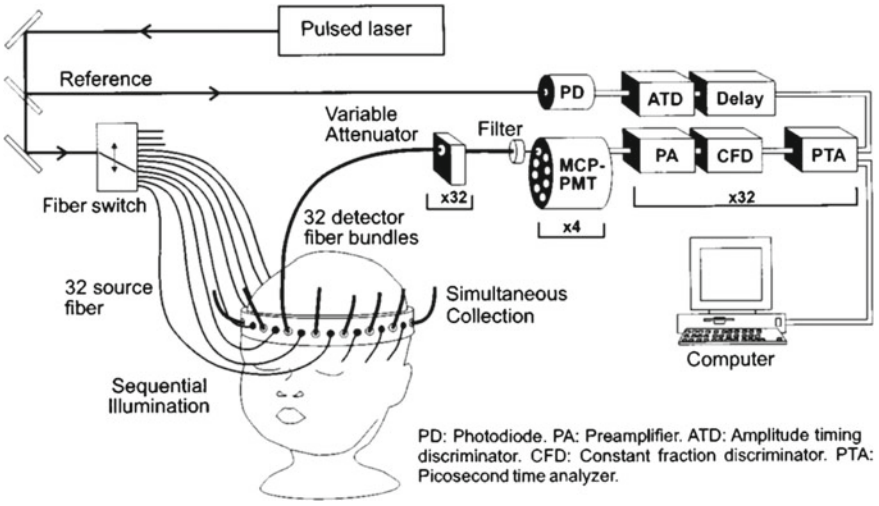

Fig. 2.12 A 32-channel time resolved OCT imaging system. After [266]

scans per second [237, 245]. The increased axial scan rate results in approximately 50 times faster data acquisition rates in practice.

OCT scanning can detect a number of eye diseases at their initial stages (sometimes years before symptoms become obvious), making treatment much more effective and reducing the chances of irreversible damage. For example, it can help provide early detection or rule out diseases such as glaucoma, macular degeneration and diabetic maculopathy. Macular hole disease is associated with a hole in the retina that can result in deterioration of vision. Prior to treatment, the loss of vision can vary depending on the size of the hole. This is further illustrated in Fig. 2.12. A case of age-related macular degeneration is illustrated in Fig. 2.14. Deterioration of the macula can interfere with a patient's central vision because it affects the part of the retina responsible for detailed central and colour vision.(Fig. 2.13)

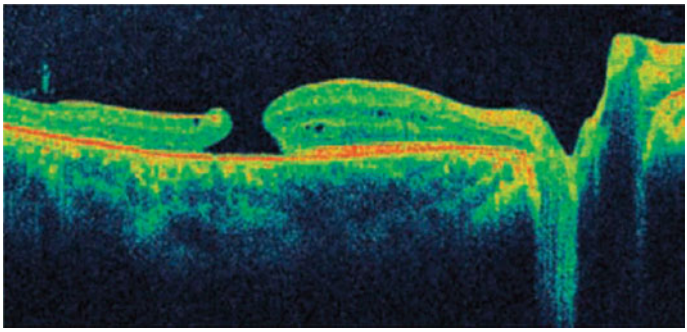

Fig. 2.13 Illustration of typical macular hole case, the hole in the retina that can result in deterioration of vision

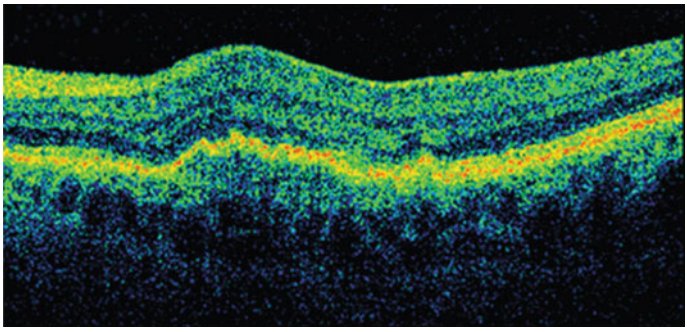

Fig. 2.14 Illustration of a case of macular degeneration. The condition is associated with a partial or complete loss of a patient's central vision

2.1.9 Alternative Multichannel and MEMS Based OCT Imaging Modalities

Beyond the applications of OCT described in the previous sections, there are also alternative multi-channel implementations which are particularly useful to biomedical imaging e.g. for the visualization of increased vascularization in mammograms as well as the detection of abnormalities in infant brains [259]. Using Ti:sapphire lasers or alternative fibre lasers (e.g. ytterbium-doped femtosecond fiber lasers as well as large-mode-area fibre based systems) [260, 261] which can achieve high-power using chirped-pulse amplification techniques [262, 263] to generate femtosecond or few picosecond pulses, the signal-to-noise ratio of such imaging techniques has been steadily improving over the past 20 years. These multi-channel techniques use transmitted light between pairs of points to perform reconstruction of an arbitrary three-dimensional distribution of internal scatterers and absorbers. As this type of imaging suffers from significant scattering, the Radon transform [264] which is used in MRI, may not be used and alternative algorithms for the extraction of the effective refractive index and scattering coefficients have been developed [265, 266]. An excellent example of such imaging system is the one developed at University College London known as the multichannel optoelectronic near-infrared system for time-resolved image reconstruction (MONSTIR). This system has now evolved to provide multispectral imaging at 4 wavelengths between 650 and 900 nm [122] and has significant potential for generating functional images of newborn brain [123].

This multi-spectral approach to diffuse optical imaging leads to the generation of independent images of changes in concentration of oxyhemoglobin and deoxyhemoglobin so current efforts focus on the development of data-driven approaches for optimum wavelength selection [124]. Another interesting aspect of current work in

this area is the application of spatio-temporal regularisation techniques [125] which can provide real-time three-dimensional dynamic reconstruction of the optical properties of a hemispherical infant head phantom, taking into consideration the moving absorption as well as scattering targets. These signal processing techniques are of much relevance to the THz transient tomography community, if adapted accordingly so that the THz scattering component associated with the shortest wavelengths of the broadband signal is significantly suppressed.

Finally, it is worth noting that alternative implementations of OCT using micro-electromechanical systems for endoscopic applications [126, 127] are also rapidly evolving and have important biomedical applications e.g. in bladder cancer diagnosis [127]. Such techniques also show significant potential for further integration with alternative complementary imaging techniques such as photoacoustic microscopy and ultrasound imaging [128, 129]. The development of new image processing algorithms that can perform de-noising, image segmentation as well as classification that can lead to improved spatio-temporal correlations for improved functional imaging across different tissues is a unifying theme that will be discussed in the following chapters.

http://www.springer.com/978-3-319-57026-6

Pattern Classification of Medical Images: Computer Aided Diagnosis

Yin, X.-X.; Hadjiloucas, S.; Zhang, Y.

2017, XIV, 218 p. 87 illus., 67 illus. in color., Hardcover
ISBN: 978-3-319-57026-6